 doi:10.20944/preprints201901.0154.v1

Article

Simple method of creating hydrophobic surfaces based on modified MW-CNTs

Marat Eseev [1*], Andrey Goshev[1*] and Sergey Kapustin[1]

[1] Northern Arctic Federal University named after M.V. Lomonosov, Severnaya Dvina Emb. 17, 163002, Arkhangelsk, Russia

* Correspondence: m.eseev@narfu.ru, agoshev@hotmail.com; Tel.: +7–902–190–5195

Abstract: The creation of hydrophobic, antifreeze and self-cleaning coatings is currently being pursued by many industrial sectors. The potential applications include the production of liquid and gas separators and filters, new materials, optical and microelectronic devices, and textiles and clothing. These coatings will also have wide application in the construction and automobile industries, shipping, and energy and agricultural sectors.

The article proposes a simple approach to the creation of superhydrophobic and antifreeze coatings, by applying powder from multi-walled carbon nanotubes (MW-CNTs) to the sample surface. This method enables combination of the necessary factors: low surface energy, micro–nano-roughness and hierarchical multi-scale. The authors investigated the dependence of the wetting angle of such a surface on the time, type and degree of functionalization. The electrophysical properties of modified MW-CNTs were studied over wide frequency and temperature ranges. This method of obtaining hydrophobic coatings differs from currently available methods in that it is simpler to prepare, is of lower cost and has less environmental impact. The proposed approach can be used to create superhydrophobic coatings that have the additional function of removing static charge and therefore reducing surface heating, and which can be used in the field of energetics for protection against the freezing of wind turbine blades and aircraft surfaces.

Keywords: Multi-walled carbon nanotubes (MW-CNTs), xerogel, functionalization, superhydrophobic coatings, contact wetting angle, electrophysical properties, conductivity.

1. Introduction

Superhydrophobic surfaces are a contemporary topic; because such coatings are resistant to pollution, icing and corrosion, their use reduces maintenance and repair costs and thus prolongs product lifetimes. Thus, the successful development of self-cleaning superhydrophobic materials is a very important technological task, and should reduce wear and corrosion caused by interaction of a surface with moisture, and increase the service life of the material.

Superhydrophobic coatings have a wide range of applications in such areas as: self-cleaning surfaces, microscale liquid devices, separators, textiles, automotive parts, construction, agriculture, energy (wind generator protection from freezing, self-cleaning solar cells), optical and microelectronic devices (cameras, mobile phones, lenses, optical sensors), and in the maritime industry (anti-fractional and anticorrosion protection of propeller screws).

Thomas Jung first considered and described the forces acting on a drop of liquid more than two hundred years ago [1]. The creation of a superhydrophobic surface became relevant about two decades ago, thanks to the work of Wenzel, Cassie and Baxter. Since then, the development of new types of superhydrophobic surfaces has become increasingly relevant, and research continues [2–5] using new materials, nanoparticles and polymers. Various methods for obtaining this kind of surface

 doi:10.20944/preprints201901.0154.v1

are used, including chemical etching, lithography, deposition of nanoparticles and the use of the "slippery porous surfaces impregnated with a liquid" (SLIP) effect; some of them are presented in a brief overview below.

It is well established that three factors are needed to create a superhydrophobic surface: low surface energy, micron–scale roughness and hierarchical multi-scale [2, 5, 6, 7, 8]. The criterion for superhydrophobicity is a wetting angle of more than 150°. In nature, this effect occurs when dew appear on certain types of plant leaves and is called the "lotus effect" (although in the case of the lotus leaf itself, the wetting angle is 152 °).

A study of the water-repellent properties of plant leaves was presented in [5]. It was shown that the hydrophobicity of some leaves could be explained by taking into account different scales of surface roughness, and sometimes additional elastic structures covering the leaf surface. Both concepts were illustrated by two different types of plant leaves, as well as a modelled surface with aggregates of carbon nanotubes on it. The natural superhydrophobicity of the lotus leaf itself is associated with the presence of an innate hydrophobic epicuticular wax and isotropic micron–large-scale roughness of leaf hairs (papillae) [9, 10].

In [11], the authors produced an artificial lotus leaf on a cotton surface. They used pure multi-walled-carbon nanotubes (MW-CNT) and modified CNTs (PBA–g–MW-CNT) as building blocks to mimic the surface texture of a lotus leaf. The resulting wetting angle was greater than 150 °.

The chemical method of obtaining hydrophobic surfaces is based on the preparation or modification of the surface by non-polar chemical functional groups. In [12], the authors associate surface hydrophobicity with the presence of hydroxyl, carboxyl or sulfa groups, while hydrophobicity depends on the presence of non-polar groups, such as the methyl group. The application of such a coating is a technologically simple process, but this approach does not enable a high wetting angle to be achieved.

The authors of [3] obtained a contact wetting angle of 161 ° using a vertically oriented array of carbon nanotubes 10–15 μm in length (a nanotube forest). However, the position of the droplets was unstable and they seeped into the CNT array within a few minutes. Unfortunately, growing a nanotube forest is a complex task requiring specialist equipment, and a nanotube forest is only suitable for a limited number of surfaces. However, there are other methods of obtaining similar surfaces.

Electrochemical and chemical methods of metal surface etching before the formation of structured nanodefects were presented in [4, 13]. In [4] the authors investigated the change in the contact angle of water and the surface roughness with the time of aluminum etching with HCl solution. The maximum wetting angle did not exceed 138 °. Other methods include the creation of micro–nano irregularities on the surface of a hydrophobic sample [14, 15], use of etching and lithography [16], and also combinations of these methods [11, 15, 17]. To obtain a hydrophobic surface, the authors of [17] used sieves of a special shape and composition as a pattern matrix, which were applied to the surface of polypropylene. The result was a superhydrophobic surface with a contact wetting angle of 152 °, which is the same as the lotus leaf.

Yet another way to create a superhydrophobic surface has been reported [13]; here the authors used the etching process on a polycrystalline copper sample. The hydrophobicity of the sample was increased by using fluorine–carbon modified with thiol groups, which gave a contact angle of 171 °. The whole process of precipitation, etching and cleaning took about 4 hours.

 doi:10.20944/preprints201901.0154.v1

The most widely known and industrially feasible method today uses silicon nanoparticle deposition (to create a hierarchical multi-scale) with subsequent temperature fixation and chemical treatment (to reduce surface energy), for example, perfluorooctyltriethoxysilane, as reported in [8]. In [15] a superhydrophobic coating was obtained by deposition of modified silica nanoparticles on a polyurethane emulsion. In [18], other types of silicon nanoparticle modification were used to obtain a superhydrophobic surface based on a polymer and a hydroxylated nanocolloidal silicon suspension.

In [19] high wetting angles and hierarchical multi-scale were observed on a metal surface after its exposure to a femtosecond laser pulse.

The formation of ice on various infrastructures is a serious barrier to ensuring their energy-efficient and safe operation. Researchers have shown that nanomaterials form the basis of coatings that are being adopted to provide anti-frost protection for various types of infrastructure. Nanomaterials allow changes to be made to surface morphology, providing the roughness required to create superhydrophobicity and ensure mechanical strength [20].

The original method of obtaining anti-icing surfaces was proposed in [6]. The authors described a new approach to the creation of functional coatings using fossil diatomaceous earth particles coated with a thin layer of graft polymer chains. Particles glued to the epoxy resin surface formed mechanically stable superhydrophobic coatings.

In [21] the authors proposed a strategy for implementing dynamic control of a surface microstructure using a shape memory polymer (SMP). They obtained a surface that could reversibly switch between two superhydrophobic modes: an isotropic state similar to a lotus leaf and a rice-leaf-like anisotropic wetting state. The concept of switching between modes can be easily extended to various control signals, for example, light, magnetic and electric.

Inspired by the idea of repulsing colliding liquids in natural systems such as the “Nepenthes jar”, the authors of article [22] produced synthetic liquid-repelling surfaces impregnated with a special lubricant. Such surfaces are called “slippery porous surfaces impregnated with a liquid” (SLIPS); they consist of a lubricating fluid film fixed by a micro–nanoporous substrate. The contact angle is mainly determined by the adhesion of the lubricant and the liquid, which allows small sliding angles to be achieved.

Note that, despite the abundance of methods for obtaining highly hydrophobic surfaces, few have seen industrial application. This is the reason why a simple and affordable method – entailing low production costs and having a low environmental impact – is sought.

2. Materials and Methods

Carbon nanotubes are non-polar hydrophobic structures with a high aspect ratio. They are strong, wear-resistant objects; they have high thermal and electrical conductivity, as well as being prone to the formation of porous agglomerates with developed surfaces. Moreover, CNTs can be modified by various functional groups to provide directional derivatization of the surface and affinity for a binder material. Such characteristics enable the required hydrophobic properties of the object to be selected and open up a wide field for experimentation. Currently the lowest cost, and, therefore, the most popular (in the applied sense) method for the synthesis of CNT is the chemical vapor deposition method (CVD): the cost of MW-CNTs obtained by this method could be less than two

 doi:10.20944/preprints201901.0154.v1

dollars per gram, which in turn opens up opportunities for these CNTs to be applied to the commercialization of materials.

To prepare and study the properties of highly hydrophobic surfaces, the we used the MW-CNTs obtained by the CVD method; their characteristics are shown in table 1.

Table 1. Characteristics of MW-CNTs of various grades from the manufacturer.

Characteristic	**Taunit–M**	**Taunit–MD**
Outer diameter, nm	10–30	8–30
Internal diameter, nm	5–15	5–15
Length, μm	≥2	≥20
Total amount of impurities, %	≤5	≤5
Specific surface, m^2 / g	≥270	≥270
Bulk density, g / cm^3	0.025–0.06	0.025–0.06

2.1 Xerogel preparation

To study the dependence of the wetting angle on the size of the CNT agglomerate, powder was prepared from ground xerogel based on carbon nanotubes. The advantage this kind of approach is that the strength of the powder's micrograins and constancy of its morphology make the powder only weakly dependent on external influences.

The xerogel was prepared from Taunit–M and Taunit–MD nanotubes. The high aspect ratio of CNTs allows the production of a xerogel even without the use of a binder polymer. For this purpose, a dispersed solution of MW-CNT in isopropyl alcohol was prepared in a ratio of 1:1 by volume. The nanotubes were then subjected to ultrasonic dispersion with constant stirring for an hour. The resulting mass was dried for 5–6 days at room temperature under vacuum. At the final stage, the xerogel was cut into small pieces and dried at 80C for about 5 hours. To obtain minute fractions, the xerogel was ground in a mortar and sieved through a set of sieves. The sifted material was then applied to carbon tape. The contact angle and slip angle were measured many times, and the average values for each series of samples obtained.

2.2 Functionalization of CNT with nitric acid

It is known that, due to the specific chemical structure of the sp^2 hybrid bond, as well as π–electron orbitals, pure CNTs do not interact well with polar groups and, through the Van der Waals interaction, twist and form aggregates up to micron size [23]. These facts complicate their functional use, both in pure form and as a dispersed phase in a composite, since this causes the electrophysical, mechanical and hydrophobic properties of the CNT to deteriorate. The authors have written a number of papers on possible options for cleaning and modification of CNTs [24, 25].

To obtain and study hydrophobic coatings, the authors of [25] used a sample of Taunit–M MW-CNTs obtained by the CVD method. In our work, purification was carried out through

 doi:10.20944/preprints201901.0154.v1

functionalization of the CNTs with nitric acid (HNO_3) at a temperature of 120C, followed by decantation and drying, as described in [25]. The processing time in the liquid phase of the acidic medium was 10, 30, 40, 60, 90, 180, 240 minutes, respectively. In order to measure the wetting angle, the obtained samples of CNTs were deposited as a thin layer on the surface of carbon tape. The hydrophobic properties of the functionalized nanotubes (f-MW-CNTs) were investigated by analyzing them for defects, amorphous carbon phase and the relative number of grafted carboxyl groups using Raman spectroscopy, conductometric titration and dielectric relaxation spectroscopy.

2.3. Wetting angle measurements

The hydrophobicity of the final product surface was measured on a Drop Shape Analyzer — a DSA20E (EasyDrop, from KRÜSS Germany). The contact angle was measured by the lying drop method.

2.4 *Raman spectroscopy*

Confocal micro-Raman spectroscopy was carried out using an NTEGRA Spectra (NT-MDT, Russia) set up in back-scattering mode at room temperature with a 632.8 nm (1.96 eV) excitation laser wavelength. The excitation laser power was kept below 1 mW/cm^2 to avoid overheating the sample. Scattered light spectra were collected with a CCD camera for 5 min each.

2.5 Conductometric titration method

Determination of carboxyl groups was performed by direct conductometric titration with a solution of KOH at a concentration of 1 mmol / l. A suspension of 200 mg f–CNT in 50 ml of distilled water was titrated with a solution of KOH from a microburette. The conductivity of the solution at the time of titration was measured with a SevenCompact © conductometer (Mettler Toledo, USA). In the initial suspension used in this method, only H^+ and R–COO– ions are present, and when KOH is added, the highly mobile H^+ ion is replaced by K^+, which has a lower conductivity. Thus, when KOH is added up to the equivalence point, the electrical conductivity of the solution decreases, and then increases due to the appearance of free hydroxide ions in the solution. The calculation of the carboxyl groups' content was carried out according to the volume of the added titrant; at the equivalence point the number of carboxyl groups is equal to the amount of the added KOH.

2.6 Dielectric relaxation spectroscopy

'To determine the electrophysical properties,, we used dielectric relaxation spectroscopy performed on a Novocontrol Concept 80 (Novocontrol Technologies GmbH & Co. KG, Germany): each f-MW-CNT sample was placed in a capacitor cell, to which was applied an alternating electromagnetic field over a frequency range of 0.01–10^7 Hz at temperatures of 140–480 K.

2.6 Electron scanning microscopy

The surface morphology was investigated using a scanning electron microscope Vega 3Sem (TESCAN, Czech Republic) under an acceleration voltage of 10 kV.

3. Results and Discussion

 doi:10.20944/preprints201901.0154.v1

3.1. Hydrophobic coatings based on xerogel

Pre-prepared xerogel (see section 2.1) was applied to carbon tape. Table 2 presents the results of contact angle dependence on the different sizes of ground fractions of powder xerogel and the type of CNT.

Table 2. Dependence of the contact angle on the size of the fractions and brand of MW-CNT.

Fraction size, mm	Taunit–M			Taunit–MD		
	Contact angle dispersion	Average value of contact angle	maximum of slip angle	Contact angle dispersion	Average value of contact angle	maximum of slip angle
0.500 – 0.315	28.6	140	180	72	108	180
0.315 – 0.215	1,56	143	47	17,3	132	180
0.215 – 0.140	1,40	145	30	3,96	149	9
0.140 – 0.125	1,50	145	25	3,58	147	9
0.125 – 0.100	0,25	146	11	0,98	151	5

Table 2 shows that maximum wetting angles of 146 ° and 151 ° were achieved for xerogel aggregates with a maximum fraction size of 0.1 mm prepared from Taunit–M and Taunit–MD, respectively. A strong dependence of the contact angle on the size of the fraction was observed for Taunit–MD, which we associate with morphological features and the aspect ratio of the samples. The variance characterizing the measure of the spread of the results also decreased with decreasing fractions size. Figure 1 illustrates the features of the surface and hierarchical multi-scale xerogel prepared from Taunit–MD. Large fractions, comparable in size with a drop, can be seen, which would have adversely affected the hydrophobic properties of the surface. Sifting out these large fractions and increasing the homogeneity of the sample enabled the contact wetting angle of the surface to be increased, which conferred superhydrophobicity on the sample.

Preprints (www.preprints.org) | NOT PEER-REVIEWED | Posted: 16 January 2019 doi:10.20944/preprints201901.0154.v1

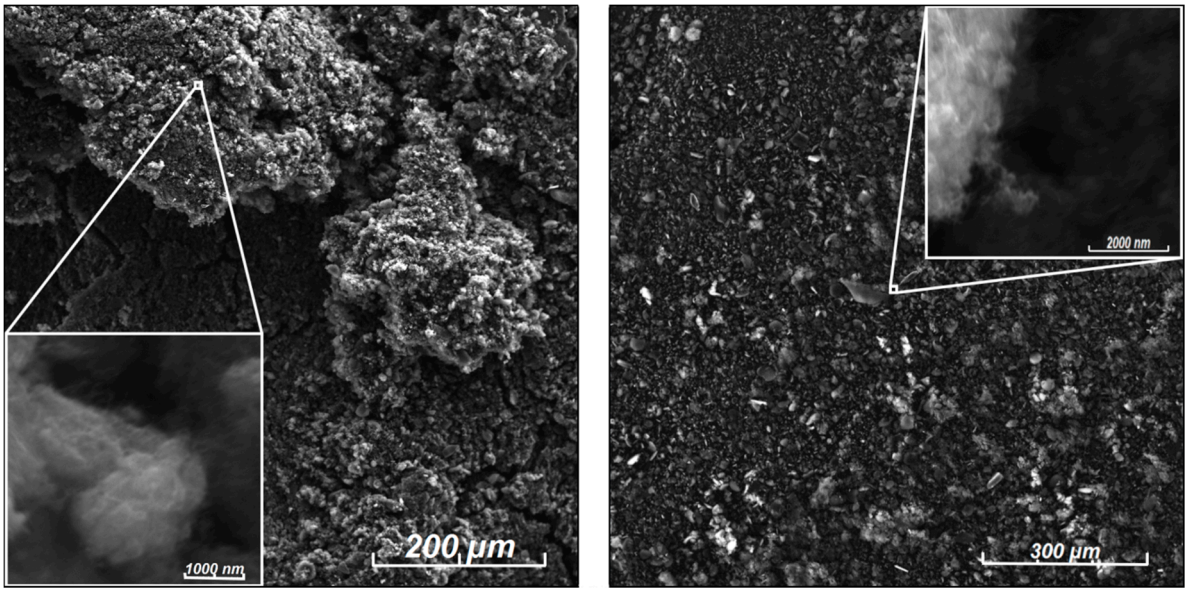

Figure 1. Scanning electron microscopy (SEM). Image of the xerogel from CNT brand Taunit–MD. Maximum fraction is 0.1 mm (right hand side) and 0.5 mm (left hand side).

The experiment made it possible to reveal the role of the particle size of CNT agglomerates in creating a highly hydrophobic surface. This coating can be sprayed on to virtually any surface without the use of special equipment.

3.2 Effect of chemical oxidation on MW-CNT hydrophobicity

To study the effect of acid treatment time on MW-CNT brand Taunit–M, we prepared a series of samples (see section 2.2) with a small time interval of functionalization (up to 90 minutes), as well longer time intervals (three and four hours) for comparison. We investigated the dependence of the wetting angle on the time of oxidation. Figure 2 shows photographs of a drop on the surface of a prepared coating for some functionalization times.

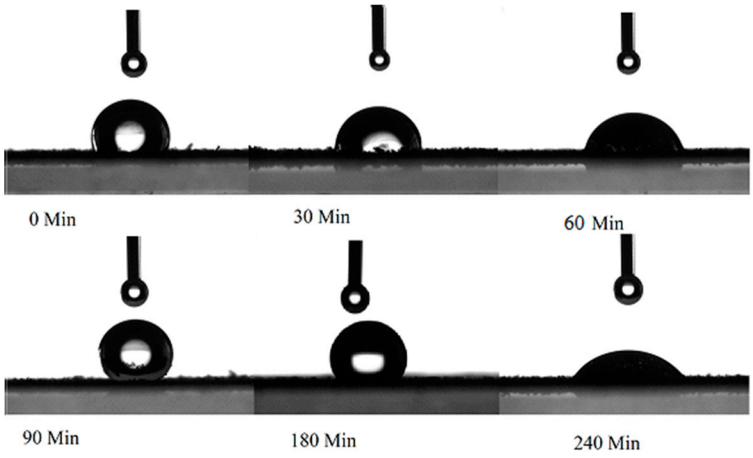

Figure 2. Photographs of the wetting angle of the drop.

Preprints (www.preprints.org) | NOT PEER-REVIEWED | Posted: 16 January 2019 doi:10.20944/preprints201901.0154.v1

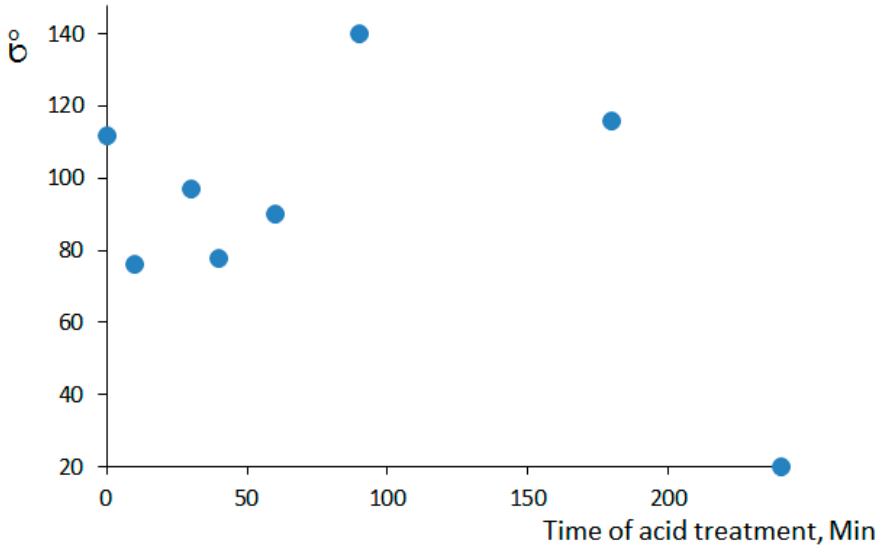

Figure 3. Dependence of wetting angle on time of MW–CNT functionalization.

From the above results, it follows that the contact angle and, consequently, the hydrophobic properties of CNTs do not show linear dependence on the time of acid treatment. In the first 10 minutes of functionalization, the contact angle decreased from 112° to 76°; over the next 40 minutes of functionalization (total time 50 min), the angle oscillated around 88°, which we associated with intensive cleaning of the amorphous carbon phase and oxidation of the catalyst particles. The maximum wetting angle was reached at 90 minutes of oxidation, and was 140 °; the angle then decreased to 20 ° at 240 minutes (see Figure 3). We consider that the nonlinearity of the function σ ° (t) of the wetting angle from the time of oxidation with nitric acid to be due to the removal of the CNT from the amorphous carbon phase during the initial stage and up to 100 minutes, and the subsequent grafting of polar functional groups –COOH on to the CNTs'. To confirm our hypothesis and establish the processes occurring at the initial stages of the oxidation of HNO_3, a series of more specifying experiments was carried out.

Figure 4 shows the dependence of the Raman spectra, and the intensity ratio of the peaks D and G, on processing time.

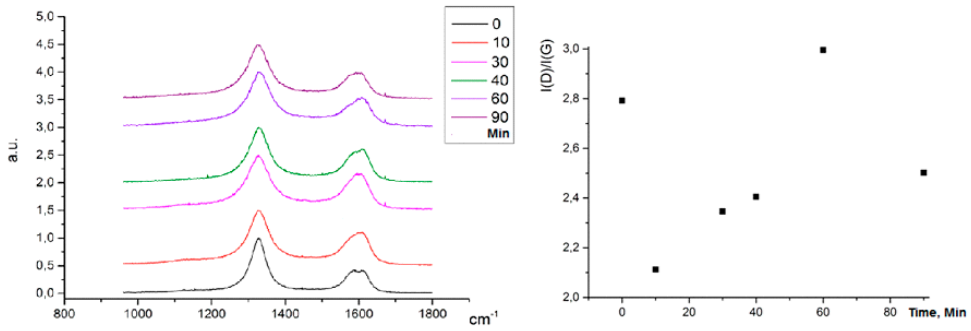

Figure 4. Raman spectra (left) and the degree of imperfection of CNTs (right), depending on the functionalization time.

Peaks in the range from 1200 cm^{-1} to 1800 cm^{-1} are first order. The most informative of them are the following (Fig. 4): band D (disorder) is located at ~ 1325 cm^{-1} and G (graphite) at ~ 1580 cm^{-1}. In

Preprints (www.preprints.org) | NOT PEER-REVIEWED | Posted: 16 January 2019 doi:10.20944/preprints201901.0154.v1

addition, the D' region is present at a higher frequency near the G band at ~ 1620 cm^{-1}. In general, the D range in the sp^2 spectra of Raman scattering is explained by disordered carbon, vacancies, grain boundaries, amorphous carbon, or any other structures of finite size that reduce crystal symmetry [27]. To assess the structure of graphene nanotube layers, as well as structural damage during oxidation, the intensity ratio I_D/I_G of the D band and the G band are used, where I_i is the intensity of the ith peak. These relationships allowed us to estimate the degree of defectiveness of f-MW-CNT depending on the time of acid treatment.

As noted in [26, 27], an exact correlation between the individual contributions of specific defects and the corresponding Raman signal has not yet been established for MW-CNT, which makes data analysis based only on the Raman spectra very difficult, especially when the oxidation time intervals are small. Therefore, to enable a more detailed analysis of the effects of acid treatment and its influence on nanotube structure (cleaning, defect formation, COOH–group grafting), we conducted a spectroscopic study by conductometric titration as well as by Raman spectroscopy (see section 2.5).

Figure 5 presents the results of conductometric titration for functionalization times up to 90 minutes. For oxidation times of 180 and 240 minutes, the number of detected groups increased by an order of magnitude.

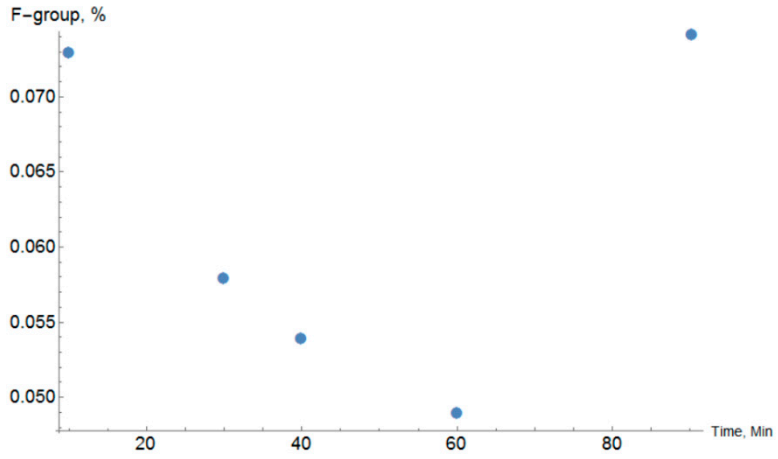

Figure 5. Dependence of carboxyl group concentration on oxidation time (by sample weight) .

The initial CNT defect (I_D / I_G) = 2.8 during the first 10 minutes of oxidation drops sharply to 2.1, and then begins to increase, reaching a maximum of 3.0 at 60 minutes of oxidation. The results of conductometric titration show that the number of functional groups decreases with increasing oxidation time, having a minimum at 60 minutes of processing. Further, the degree of functionalization increases. Comparison of the Raman spectroscopic data and the conductometric titration method made it possible to conclude that the initial defects of CNT are caused by the presence of amorphous carbon, which is oxidized at the initial stages of functionalization (the first 30 minutes) during intensive interaction with acid. The next stage – the combustion of catalyst clusters and the opening of the MW-CNT cavity – takes place within a time interval of 30–60 minutes, after completion of which there is maximum defectiveness (I_D/I_G ratio) of CNTs and a minimum in the detected COOH group number. We therefore conclude that the small times of functionalization (up to an hour) are in the nature of the MW-CNT cleaning. The grafting processes of f-groups begin to dominate on the surface layers of CNT at stages of 100 minutes' duration and longer. We note that the grafting groups' number increases linearly, reaching 0.22 and 0.32% at 180 and 240 minutes of

Preprints (www.preprints.org) | NOT PEER-REVIEWED | Posted: 16 January 2019 doi:10.20944/preprints201901.0154.v1

oxidation, respectively. After four hours of oxidation, the number of polar groups on the periphery of the CNT becomes sufficient to make carbon nanotubes hydrophilic. This is also confirmed by measurement of the wetting angle (Fig. 3.).

3.3 Investigation of the electrophysical properties of MW-CNTs

Dielectric relaxation spectroscopy over a wide temperature range is of interest both for diagnostic purposes (the grafted groups appear in the high-frequency region in the conductivity–frequency dependence) and in the applied sense. It is worth noting that anti-icing surfaces based on CNTs allow pass electric current to through them, contributing to self-cleaning of the surface from the ice crust by heating it. In this case, CNTs provide conductivity of anti-icing coatings and high thermal conductivity during heating of the surface due to the creation of alternating electric fields in the material and the excitation of eddy electric currents.

Figure 6 shows three-dimensional graphs of conductivity versus frequency and temperature. Note that the frequency dispersion for samples is absent across the entire temperature range, both for pure CNTs and for short functionalization times (up to 60 minutes). The presence of functional groups is well monitored by this method in the high-frequency region, where, starting with frequencies of the order of 106, the conductivity decreases sharply. Moreover, the critical frequency at which the transition occurs depends on the number of grafted functional groups, decreasing with the growth of the latter.

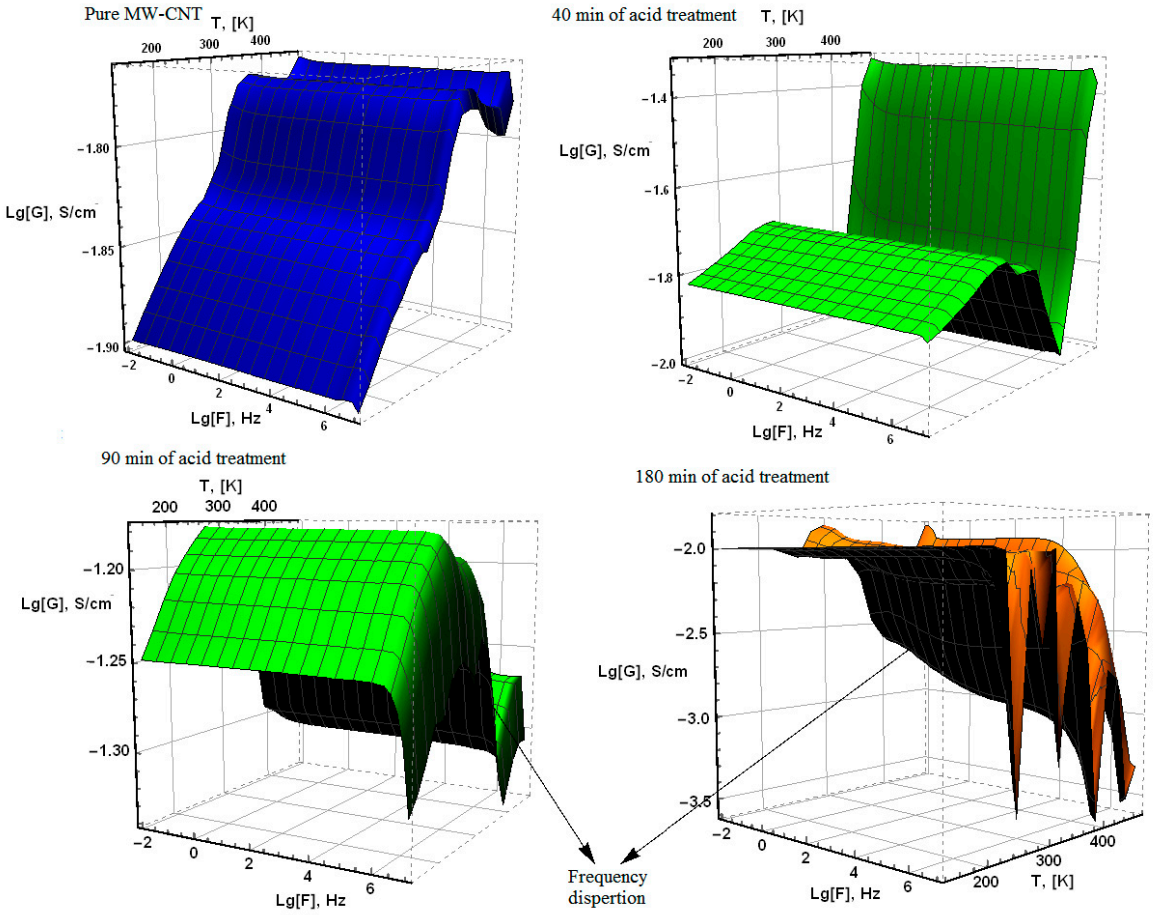

 doi:10.20944/preprints201901.0154.v1

Figure 6. Dependence of conductivity on the alternating field frequency at different temperatures for different times of functionalization.

An analysis of the data in Table 3 allows us to conclude that for small times of functionalization, the temperature dependence of conductivity in the low-frequency region is weakly expressed. The temperature dispersion of conductivity makes a significant contribution when the number of grafted carboxyl groups becomes noticeable (from three hours of oxidation). In addition, note that the maximum conductivity observed at 60 minutes functionalization time – when CNTs are cleared of the amorphous carbon phase and the number of grafted functional groups is small (see section 3.2).

Time of acid treatment	Conductivity σ *10^{-2} , [S/cm] at a frequency of 10^{-2} Hz		
	T=300 K	T=200 K	T=400 K
0	1,53	1,37	1,68
10	4,88	4,32	4,24
30	6,49	5,95	6,92
40	1,77	1,69	1,01
60	13,99	12,55	12,68
90	6,42	6,24	5,04
180	1,44	1,01	0,40

Table 3. Conductivity versus functionalization time for temperatures of 200, 300, 400 K, at a frequency of 10^{-2} Hz.

The methods we have employed in our study have allowed us to identify the processes occurring in the initial stages of acid treatment, to determine the optimal time for cleaning CNTs and to identify the relationship between the hydrophobic properties of the surface and the quality of the cleaning of MW-CNTs.

4. Conclusions

Our aim in this study was to obtain a highly hydrophobic surface by applying CNT agglomerates made from ground xerogel to carbon tape. A hierarchical multi-scale xerogel was formed by means of both CNT agglomerates at the microscale and MW-CNTs themselves at the nanoscale. This allowed us to obtain a superhydrophobic coating with a contact wetting angle near to 151°. The study of the short functionalization times of MW-CNTs showed that the initial stages (up to 90 minutes) are dominated by the process of tubes being cleaning from the amorphous carbon phase and from metal nanoparticles – the catalyst. The grafting processes of carboxyl groups become dominant after 90 minutes of oxidation. CNTs purified in this way showed an increase in the wetting angle from 112 ° (pure Taunit M) to 140 ° (the functionalization time is 90 minutes), allowing this coating to be considered highly hydrophobic. The study of conductivity over a wide temperature regime did not reveal any significant changes. This makes it possible to use such a surface for stable operation in the heating mode. Good conductivity will allow static charge to be removed, and cause induction heating of the surface. This effect can be applied, for example, to wind generator blades working under icy conditions. Note that the MW-CNTs modified in this way can be quite simply deposited on the polymer surface at the time of the glass transition phase, which increases the range of their application. The resulting material based on CNTs will possess high hydrophobic and anti-icing properties. The electrophysical properties of CNTs can also be used in the design of coatings cleared of ice during heating due to the flow of eddy currents excited in the coating material.

346

347 **Author Contributions**

348 E.M.K., G.A.A., and K.S.N. conceived and designed the experiments. G.A.A. and K.S.N. conducted the
349 experiments. E.M.K., G.A.A., and K.S.N. analyzed and interpreted the data. All authors contributed to the
350 writing and editing of the manuscript.

351

352 **Conflicts of Interest**

353 The authors declare no conflict of interest

354 **References**

355 [1] Young, T.; An essay on the cohesion of fluids. Philos. Trans. R. Soc. London, 1805, 95, 65-87,
356 DOI:10.1098/rstl.1805.0005.
357 [2] Roach, P.; Shirtcliffe, N.J.; Newton, M. I. Progess in superhydrophobic surface development, Soft
358 Mat., 2008, 4 , 224–240, DOI: 10.1039/B712575P.
359 [3] Kenneth, K. S. Lau; Kenneth, B. K.; at all., Superhydrophobic Carbon Nanotube Forests. Nano
360 Let., 2003, 3, 1701 – 1705, DOI:10.1021/nl034704t.
361 [4] Lafuma, A.; Quere, D. Superhydrophobic states. Nat. Mat., 2003, 2, 457–460, DOI:
362 10.1038/nmat924.
363 [5] Otten, A.; Herminghaus, S. How plants keep dry: a physicist's point of view. Langmuir, 2004, 20,
364 2405–2408. DOI 10.1021/la034961d.
365 [6] Puretskiy , N.; Chanda, J.; Stoychev G.; Synytska, A. Anti–Icing Superhydrophobic Surfaces
366 Based on Core–Shell Fossil Particles, Adv. Mat. Int., 2015, 2, 1500124 - 1500131 DOI:
367 10.1002/admi.201500124.
368 [7] Sunyoung, S.; Dongyoung, K.; Kang, B.; Myunggyu, C.; at all. A stable super–hydrophobic and
369 self–cleaning all surface formed by using roughness combined with hydrophobic coatings, Molec.
370 Cryst. and Liq. Cryst., 2014, 6, 9–16, DOI: 10.1080/15421406.2014.944358.
371 [8] Junpeng, L.; Janjua, Z. A., at all. Super–hydrophobic/icephobic coatings based on silica
372 nanoparticles modified by self–assembled monolayers, Nanomat., 2016, 6, 232 - 233 ,
373 DOI:10.3390/nano6120232.
374 [9] Howarter, J.A.; Genson, K. L. Youngblood, J. P. Wetting behavior of oleophobic
375 polymer coatings synthesized from fluorosurfactant–macromers. ACS Appl. Mater.
376 Interfaces, 2011, 3, 2022–2030, DOI: 10.1021/am200255v
377 [10] Howarter, J. A.; Youngblood, J. P. Self–cleaning and next generation anti–fog surfaces and
378 coatings, Macr. Rap. Com., 2008, 29, 455–466. DOI: 10.1002/marc.200700733
379 [11] Liu, Y.; Tang, J.; Wang, R.; Lu, H.; Li, L.; Kong, Y.; Qi, K.; Xin, J. H. Artificial lotus leaf structures
380 from assembling carbon nanotubes and their applications in hydrophobic textiles. J. Mater. Chem.,
381 2007, 17, 1071–1078. DOI: 10.1039/b613914k
382 [12] Kumar, S.S.; Manik G. Recent progress in super hydrophobic/hydrophilic self–cleaning surfaces
383 for various industrial applications: a review, Pol.–Plast. Tech. and Eng., 2018, 1932-1952, DOI:
384 10.1080/03602559.2018.1447128
385 [13] Mumm, F.; Van Helvoort, A. T. J.; Sikorski, P. Easy route to superhydrophobic copper–based
386 wire–guided droplet microfluidic systems. ACS Nan., 2009, 3, 2647–2652, DOI: 10.1021/nn900607p

[14] Rao, A.V.; Latthe, S.S.; Nadargi, D.Y.; Hirashima, H.; Ganesan, V. Preparation of MTMS based transparent superhydrophobic silicafilms by sol–gel method. J. Coll. Inter. Sci., 2009, 332, 484–490. DOI: 10.1016/j.jcis.2009.01.012

[15] Xiaoli W.; Faxing Z. Surface and mechanical properties of anorganic–inorganic super–hydrophobic coating using modified nano–SiO_2 and mixing polyurethane emulsion as raw materials, Jou. of Adhes. Sci. and Tech., 2018, 32, 1809–1821, DOI: 10.1080/01694243.2018.1449574

[16] Gnanappa A.K.; Gogolides, E.; Evangelista F.; et al. Contact line dynamics of a superhydrophobic surface: application for immersion lithography. Micro fluid Nanofluid., 2011, 10, 1351–1357, DOI: 10.1007/s10404-010-0762-5

[17] Si-Si Z.; Zi–Sheng G.; Yong P. Poly.–plas. Tech. and engin., 2012, 51, 845–848, DOI: 10.1080/03602559.2012.671417

[18] Polakiewicz, A.; Dodiuk, H.; Kenig. S.; Super–hydrophilic coatings based on silica nanoparticles, Jour. of Adhes. Sci. and Tech., 2014, 28, 466–478, DOI: 10.1080/01694243.2013.840978

[19] Lishi, J.; Zhong, Y.C.; et al. Femtosecond laser produced hydrophobic hierarchical structures on additive manufacturing parts, Nanomat., 2018, 8, 601-611, DOI: 10.3390/nano8080601.

[20] Laturkar, S. V.; Mahanwar P. A. Superhydrophobic coatings using nanomaterials for anti–frost applications – review. Nanosyst. phys., chem., math., 2016, 7, 650–656, DOI: 10.17586/2220-8054-2016-7-4-650-656

[21] Zhongjun, C.; Zhang, D.; at all, Superhydrophobic shape memory polymer arrays with switchable isotropic/anisotropic wetting. Adv. Funct. Mater., 2018, 28, 1705002-1750013, DOI: 10.1002/adfm.201705002

[22] Tak–Sing, W.; Sung, H. K., at al., Bioinspired self–repairing slippery surfaces with pressure–stable omniphobicity, Nat., 2011, 477, 443–447, DOI: 10.1002/adfm.201705002.

[23] Goshev, A.A.; Eseev, M.K.; Investigation of the influence of polymerization temperature on the agglomeration process of the CNT in the composite matrix, IOP Conf. Ser.: Jour. of Phys., 2017, 917, 092013-092019, DOI: 10.1088/1742-6596/917/9/092013

[24] Singer, G.; Siedlaczek, P.; at all. Acid free oxidation and simple dispersion method of MWCNT for high–performance CFRP, Nanomat., 2018, 8, 912-930, DOI: 10.3390/nano8110912

[25] Dyachkova, T.P., Rukhov, A.V., at all. Functionalization of carbon nanotubes: methods, mechanisms and technological realization. Adv. Mater. & Tech., 2018, 2, 18-41. Doi 10.17277/amt.2018.02.pp.018-041

[26] Lehman, J.H.; Terrones, M.; Mansfield, E.; Hurst, K.E.; Meunier, V. Evaluating the characteristics of multiwall carbon nanotubes. Carb., 2011, 49, 2581–2602, DOI: 10.1016/j.carbon.2011.03.028 .

[27] Brown, S.D.M.; Jorio, A.; Dresselhaus, M.S.; Dresselhaus, G. Observations of the D–band feature in the Raman spectra of carbon nanotubes. Phys. Rev. B 2001, 64, 073403—73407, DOI: 10.1103/physrevb.64.073403.